Mechanical Systems and Signal Processing 33 (2012) 181–196

Contents lists available at SciVerse ScienceDirect

Mechanical Systems and Signal Processing

journal homepage: www.elsevier.com/locate/ymssp

Improved EMD for the analysis of FM signals

Xu Guanlei [a,*], Wang Xiaotong [b], Xu Xiaogang [b], Zhou Lijia [a]

[a] Department of Ocean, Dalian Naval Academy, Dalian 116018, China
[b] Department of Navigation & Automatization, Dalian Naval Academy, Dalian 116018, China

ARTICLE INFO

Article history:
Received 30 April 2012
Received in revised form
18 June 2012
Accepted 6 July 2012
Available online 4 August 2012

Keywords:
Empirical mode decomposition (EMD)
Two-level extrema structure (TLES)
t–f Distribution
Frequency modulation (FM)
Least-squares method
Mono-component and multi-component

ABSTRACT

In this paper, an innovative algorithm of improved EMD (IEMD) has been presented for the analysis of frequency modulation (FM) signals. First, extract the first level extrema and the second level extrema to construct one two-level extrema structure (TLES). Using the locations' relations between the first level extrema and the second level extrema, what the traditional EMD does for FM signals is determined. The propositions that can help us to judge whether the multi-component can be separated well or not by EMD in practice and then tell us what the EMD will do in practice are deduced. Four cases are presented for decomposition of FM components using EMD. According to these cases, different improved methods are presented to separate the FM components that EMD fails to separate. The least-squares method is used to estimate the phase polynomials of FM components. The orthogonal relations between different components are used to estimate the optimal amplitudes of FM components. Moreover, the performance of EMD is analyzed via the multi-level extrema distribution as well, which can be used in practice for the aforehand judgement. Finally, experiments are given to show our new improved EMD.

1. Introduction

After the introduction of the empirical mode decomposition (EMD) by Huang et al. [1], EMD has become one important tool to analyze nonlinear and non-stationary signals. Recently, EMD has been widely used in filtering [2–5], image processing [6–9] and others [8–12]. EMD considers signals as "fast oscillations superimposed on slow oscillations" [13]. Therefore, the biggest difference between these decomposed oscillations is the rate of oscillating. These decomposed oscillations, called IMF by Huang et al. have some interesting properties and names. Since the mono-component is different from the IMF, some other people call the mono-component weak IMF [14]. Also, EMD has been taken as one filter bank [15] or wavelet-like expansions [16]. The key benefit of using EMD is that it is an automatic decomposition and fully data adaptive, as is the biggest feature different from the classical methods such as Fourier transform, wavelet analysis and other methods. Rilling and Flandrin [17] give the theoretical claims that when and where the two tones can be separated well using EMD, and the numerical experiments are given to support their claims. Wu and Huang [18] find that two components whose frequencies lie within an octave cannot be separated by EMD. However, up till now there have been only the theoretical claims, and still there have been no existing propositions or guidance telling one when two mono-components can be separated using EMD or not in practice.

Inspired by EMD [1] and harmonic envelope [29], from the experimental viewpoint, through the local extrema of the comprised Multi-component, one two-level extrema structure (TLES) is constructed. In addition, the relations between the

* Corresponding author. Tel.: +86 13889511675.
E-mail address: xgl_86@163.com (X. Guanlei).

0888-3270/$ - see front matter © 2012 Elsevier Ltd. All rights reserved.
http://dx.doi.org/10.1016/j.ymssp.2012.07.003

TLES and the performance of EMD are derived for the FM signals. From these relations one can know when two FM signals can be separated by EMD or not in practice. If not, these relations will tell one what EMD does.

If two FM signals cannot be separated by EMD, what should be done? Masking signals based on EMD method [19,20] has given one resolution to handle two components whose frequencies lie within an octave. However, their efficient scope is mainly limited into the signals whose frequencies are constant, not the FM signals. Because in the course of construction of masking signals they used FFT to estimate frequency components that are the stationary equivalents [19,20]. In addition, due to the nature of EMD and the obscure manner it operates, in them the so far published modifications of the initially proposed algorithm leading to performance improvement are limited, especially from the viewpoint of understanding the nature of EMD. Using the relations between the TLES and the FM signals, our new proposed methods can separate these signals well. Note our main involved object is the FM signal (its amplitude is constant) in this paper. FM signals are widely used in communication, broadcast, target detection and other signal processing fields [21–24]. Thus there is one great need to discuss the FM signals solely. Thinking about the excellent features of EMD, in this paper we will analyze the FM signals using EMD.

The following of this paper is organized as follows. In Section 2, the basics of the EMD are first recalled. Section 3 presents the two-level extrema structure (TLES) resulted from the extrema of the comprised Multi-component to be decomposed. The propositions used in practice showing in what cases the Multi-component can be separated into the FM mono-components well are proposed in Section 4. Section 5 is our improved EMD for the FM signals. Three classical tests are shown in Section 6. Finally, Section 7 concludes our work.

2. Empirical mode decomposition for FM signals

2.1. Empirical mode decomposition

The EMD involves the decomposition of a given multi-component signal $x(t)=\sum_{l=1}^{N} x_l(t)$ (where $x_l(t)=a_l\cos\varphi_l(t)$ is one FM mono-component) into a series of IMFs through the "sifting process"[1]. Given a multi-component signal $x(t)$, after the sifting operation, we have the final result of EMD

$$x(t)=\sum_{l=1}^{L} imf_l(t)+r(t) \tag{1}$$

Then perform Hilbert transform on every IMF to get the according analytic signals. Instead of differential of phases used in EMD [1], here we use the trapezoidal integration rule [25–27] to compute the instantaneous frequencies of IMFs (we use the MATLAB function *instfreq*.m [28]), and the instantaneous energies are the absolute values of these analytic signals. The instantaneous frequencies and the instantaneous energies are used for time–frequency analysis (t–f distribution). For example, Fig. 1 gives the results of two chirps' decomposition using EMD and the according t–f distribution. Compared with the t–f distribution using Wigner–Ville transform, there are no crossed terms in t–f distribution of EMD.

Ideally, we hope that $L=N-1$, $x_l(t)=imf_l(t)$ ($l=1,2,\ldots,L$) and $x_N(t)=r(t)$. Thus every IMF is one FM mono-component. However, sometimes the EMD is unable to separate these mono-components well. In many cases, the EMD will combine a few mono-components into one IMF or break one mono-component into a few parts incorporated by the frequency-adjacent IMFs respectively. To measure the performance of EMD to separate these FM mono-components, one measure is defined as

$$c(t)=\min\left(1,\max_{l=1,2}\left(\frac{\|x_l(t)-imf_l(t)\|^2_{L^2(T)}}{\|x_l(t)\|}\right)\right) \tag{2}$$

This measure is used to quantity the performance of EMD.

In order to quantity the difference between the original signal $x(t)$ and the first IMF, another measure is defined

$$c'(t)=\min\left(1,\frac{\|(x)-imf_1(t)\|^2_{L^2(T)}}{\|x(t)\|^2_{L^2(T)}}\right) \tag{3}$$

Now we review the main results of Han et al. [5] and Senroy and Suryanarayanan [20] and give the following Proposition 1. Note that in the Proposition 1 only two FM signals are involved here, $x(t)=\sum_{l=1}^{2} x_l(t)=\sum_{l=1}^{2} a_l\cos\varphi_l(t)$, the frequency $f_l(t)=d\varphi_l(t)/dt$, and the amplitudes are constant. One assumption is that $f_1(t)>f_2(t)$. More components will operate in the same manner.

Proposition 1. *EMD will do one of the three things for two FM components*: *Case* I—*Separate the two FM components well. Case* II–*Treat the two FM components as one IMF. Case* III—*EMD does something else. The theoretical claims*:

(A) *If* $a_1f_1(t)>\approx a_2f_2(t)$ *and* $3f_2(t)>\approx f_1(t)>\approx 2f_2(t)$, *the two FM signals can be separated well by EMD. This belongs to the Case* I.

(B) *If* $a_1f_1(t)>\approx a_2f_2(t)$ *and* $f_1(t)>\approx 3f_2(t)$, *the two FM signals can be separated well by EMD. This belongs to the Case* I.

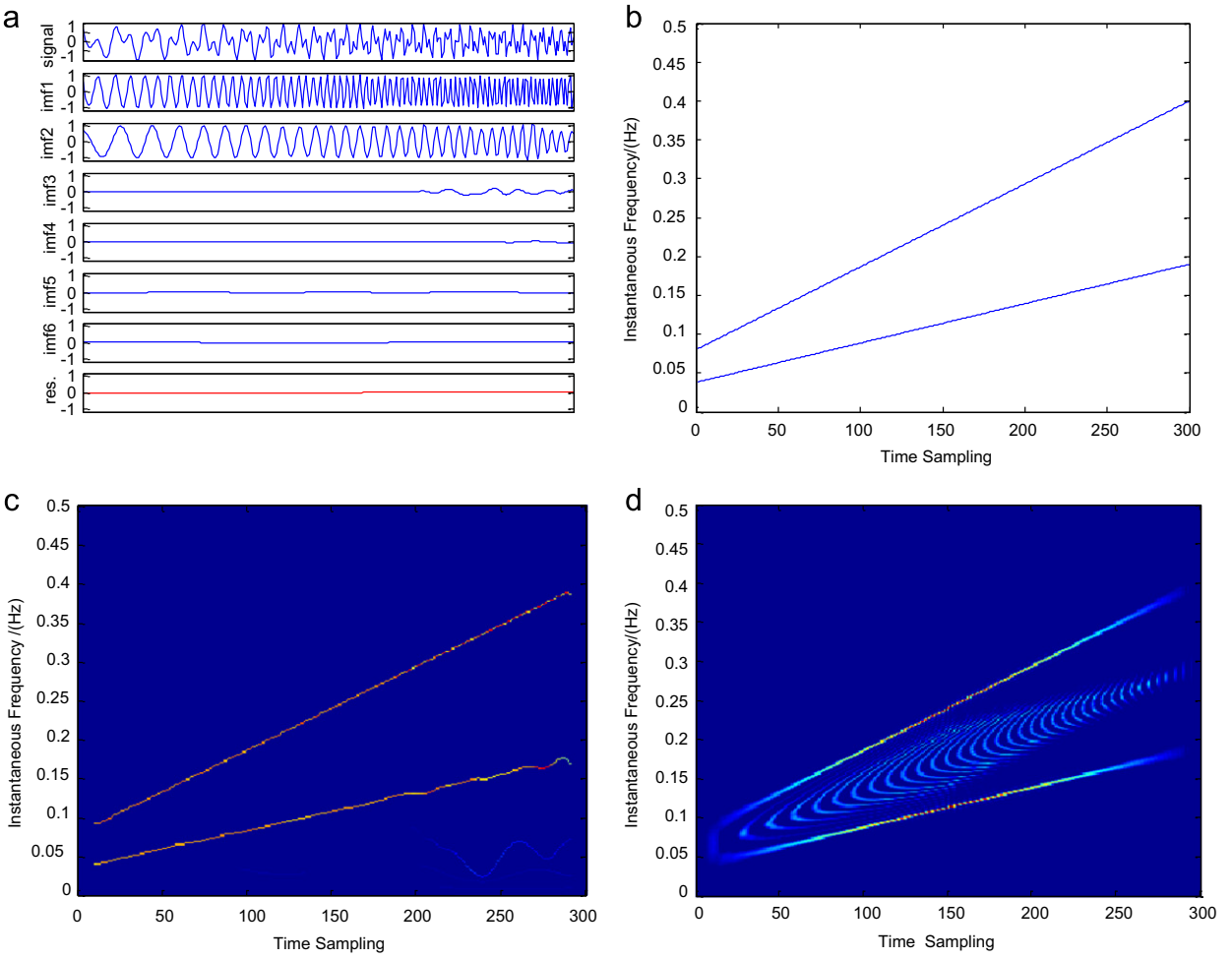

Fig. 1. The decomposition and time–frequency analysis of two linear FM mono-components (two chirps). (a) The decomposed result using EMD, (b) The real *t-f* distribution (c) *t-f* distribution of EMD (d) *t-f* distribution using Wigner-Ville transform

(C) *If* $a_1f_1(t) > \approx a_2f_2(t)$ *and* $1.5f_2(t) > \approx f_1(t) > \approx f_2(t)$, *the two FM signals can be treated as one IMF by EMD approximately. This belongs to the Case* II.

(D) *If* $a_1f_1(t) > \approx a_2f_2(t)$ *and* $2f_2(t) > \approx f_1(t) > \approx 1.5f_2(t)$, *EMD will do something else that is different from Case* I and *Case* II. *This belongs to the Case* III.

If $a_1f_1(t) > \approx a_2f_2(t)$, the extrema rate of the comprised FM component is exactly the same as that of the first FM component [5]. Here it is one common term in (A)–(D) that $a_1f_1(t) > \approx a_2f_2(t)$ holds. In Section 5.2, we discuss the case that the extrema rate of the comprised FM component is exactly the same as that of the second FM component.

2.2. AM–FM signal and IMF

Note that if $1.5f_2(t) > \approx f_1(t) > \approx f_2(t)$, two FM signals can be treated as one IMF by EMD approximately. Consider the AM–FM component

$$\begin{aligned} x(t) &= a_1\cos(2\pi f_1(t)t) + a_2\cos(2\pi f_2(t)t) \\ &= a(t)\cos(\varphi(t, f_1(t), f_2(t))) \end{aligned} \tag{4}$$

where $1.5f_2(t) > \approx f_1(t) > \approx f_2(t)$ and $a_1f_1(t) > \approx a_2f_2(t)$, a_1 and a_2 are constant magnitudes for FM signals.

For the AM–FM form, the instantaneous magnitude of $x(t)$ is

$$a(t) = \sqrt{a_1^2 + a_2^2 + 2a_1a_2\cos[(f_1(t) - f_2(t))t]} \tag{5}$$

Apply cubic spline fitting among the local extrema points of $x(t)$ to obtain two envelopes corresponding to the maximum envelope, $E_{\max}(t)$, and the minimum envelope, $E_{min}(t)$. Ideally, the true amplitude modulation of the two FM

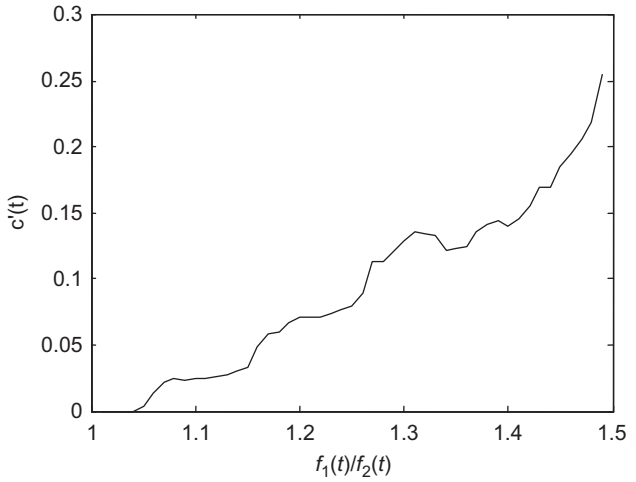

Fig. 2. The difference between the IMF and two FM components.

components is obtained from the two envelopes

$$a(t) = |E_{max}(t)| = |E_{min}(t)| \tag{6}$$

Since a_1 and a_2 are constant magnitudes, then

$$\min(a(t)) = \min\{|E_{max}(t)|,\ |E_{min}(t)|\} = |a_1 - a_2| \tag{7}$$

$$\max(a(t)) = \max\{|E_{max}(t)|,\ |E_{min}(t)|\} = |a_1 + a_2| \tag{8}$$

If the envelopes, $|E_{max}(t)|$ and $|E_{min}(t)|$, are known, a_1 and a_2 can be calculated using (7) and (8) easily.

However, there is difference between the two FM signals and the IMF when $1.5f_2(t) > \approx f_1(t) > \approx f_2(t)$. For one multi-component $x(t)=x_1(t)+x_2(t)$, where $x_1(t)=\cos(2\pi f_1(t))$, $x_2(t)=\cos(2\pi f_2(t))$, $f_1(t)=0.001$ Hz, $thd_1=2000$, $thd_2=0.01$, $0 \le t \le 10{,}000$ s. Perform EMD on $x(t)$ to obtain $imf_1(t)$, then we get the difference between $x(t)$ and $imf_1(t)$ using the measurement $c'(t)$ with the ratio $f_1(t)/f_2(t)$ changing as shown in Fig. 2. The difference will affect the estimation of the magnitudes. Therefore the initial estimated amplitudes should be optimized.

2.3. The optimization of amplitudes

For one multi-component signal $x(t)=\sum_{l=1}^{N} x_l(t)$. Now the initial amplitude estimation, $a_{l,0}$, of the component $x_l(t)=a_l\cos\varphi_l(t)$ $(1 \le l \le N)$ is known. In addition, $\varphi_l(t)$ is known. Thus the optimal estimation (or real value) of a_l is determined by

$$a_{l,opt} = \underbrace{\arg\min}_{a\in[a_{l,0}\delta_1, a_{l,0}\delta_2]} \left|\sum_t [(x(t) - a\cos\varphi_l(t))(a\cos\varphi_l(t))]\right|, \tag{9}$$

where $0 < \delta_1 < 1$, $1 < \delta_2 < +\infty$. In our paper, we set $\delta_1=0.5$ and $\delta_2=1.5$, which are empirical and sufficient.

Since these FM components have different frequencies, they are orthogonal. Therefore we have

$$\left|\sum_t [(x(t) - a\cos\varphi_l(t))(a\cos\varphi_l(t))]\right| = \left|\sum_t [(a_l\cos\varphi_l(t) - a\cos\varphi_l(t))(a\cos\varphi_l(t))]\right| \tag{10}$$

Therefore (9) holds true.

3. The TLES

For the convenience of addressing of this problem, one two-level TLES of two FM components will be given to show the mechanism of our approach. The higher-level TLES of more FM components will operate in the same manner.

For one given multi-component signal $x(t)$, whose all local maxima (minima) in the support $[0,T]$ are placed into the set LMA_1 (respectively, LMI_1):

$$LMA_1 = \left\{ x(t) : \frac{dx(t)}{dt} = 0 \ \&\ \frac{d^2x(t)}{dt^2} < 0, t \in [0,T] \right\}$$

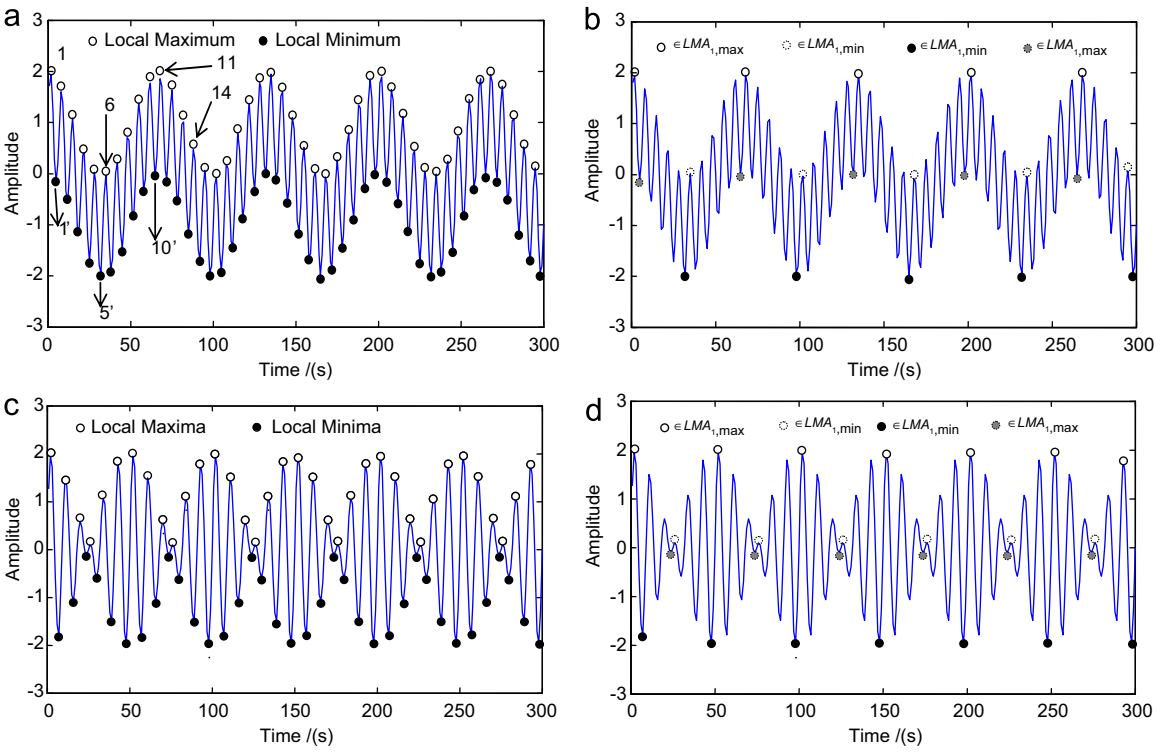

Fig. 3. The local extrema of two levels. The two FM components satisfy $a_1f_1(t) > a_2f_2(t)$ and $f_1(t) > 2f_2(t)$ in (a) and (b). The two FM components satisfy $a_1f_1(t) > a_2f_2(t)$ and $f_1(t) < 2f_2(t)$ in (c) and (d). (a) The first level extrema (b) The second level extrema (c) The first level extrema (d) The second level extrema.

$$LMI_1 = \left\{ x(t) : \frac{dx(t)}{dt} = 0 \ \& \ \frac{d^2x(t)}{dt^2} > 0, t \in [0,T] \right\}$$

Clearly, the set LMA_1 and LMI_1 are discrete data series. The signal in Fig. 3(a) and (b) is one multi-component. Its local maxima are labeled by blank circle "O", and its local minima are labeled by dark circle "●". In addition, in the set LMA_1 (LMI_1), the local maxima (minima) are labeled by numbers from left to the right in order. Since there are 45 local maxima (45 local minima), the labeled numbers is 1, 2, …, 45(1′, 2′, …, 45′) for the local maxima (the local minima respectively). For example, the number 1 (6, 11 and 14) denotes the first (sixth, eleventh and fourteenth, respectively) local maximum (from the left to the right in order). Similarly, the number 1′ (5′ and 10′) denotes the first (fifth and tenth respectively) local minimum (from the left to the right in order). For simplicity, most of the labels are not marked.

One interesting observation is that in the 45 local maxima (minima), these local maxima (minima) labeled by the numbers 1, 11, 21, 31, 41 and 6, 16, 26, 36 (1′, 10′, 20′, 30′, 40′ and 5′, 15′, 25′, 35′) are different from the others in the set $LMA_1(LMI_1)$. Comparing the 45 data with the other data, we find that the local maxima (minima) data labeled by the numbers 1, 11, 21, 31, 41 (1′, 10′, 20′, 30′, 40′) are bigger than their adjacent data in $LMA_1(LMI_1)$, and the local maxima (minima) data labeled by the numbers 6, 16, 26, 36 (5′, 15′, 25′, 35′) are smaller than their adjacent data in $LMA_1(LMI_1)$. For example, the local maximum data labeled by the number 11 is bigger than the adjacent local maxima labeled by the numbers 10 and 12. The local maxima labeled by the number 26 is smaller than the adjacent local maximum data labeled by the numbers 25 and 27. Then what will happen if we further extract new local extrema in the data series sets LMA_1 and LMI_1?

Definition 1. The data are called *the second level extrema* in the following sets:

$$LMA_{1,\max} = \{u(t_i) : \ u(t_i) > u(t_{i-1}) \ \& \ u(t_i) > u(t_{i+1}), u(t_i) \in LMA_1\}$$

$$LMA_{1,\min} = \{u(t_i) : \ u(t_i) < u(t_{i-1}) \ \& \ u(t_i) < u(t_{i+1}), u(t_i) \in LMA_1\}$$

$$LMI_{1,\max} = \{v(t_i) : \ v(t_i) > v(t_{i-1}) \ \& \ v(t_i) > v(t_{i+1}), v(t_i) \in LMI_1\}$$

$$LMI_{1,\min} = \{v(t_i) : \ v(t_i) < v(t_{i-1}) \ \& \ v(t_i) < v(t_{i+1}), v(t_i) \in LMI_1\}.$$

Clearly, the set $LMA_{1,max}$ only contains the data labeled by the numbers 1, 11, 21, 31 and 41 in Fig. 3(a). The set $LMA_{1,min}$ only contains the data labeled by the numbers 6, 16, 26 and 36 in Fig. 3(a). These data also can be seen in Fig. 3(b). With

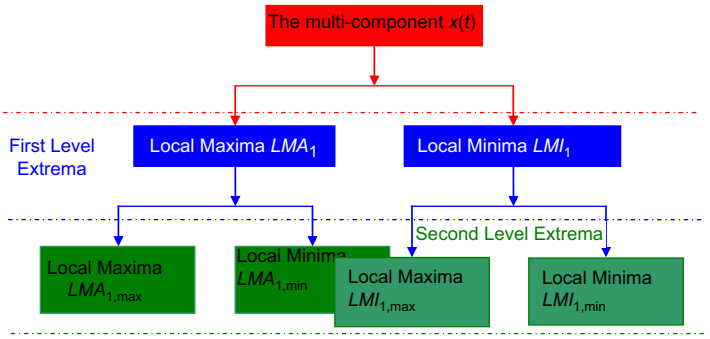

Fig. 4. Two-level extrema structure of one FM multi-component signal.

respect to the names of the second level extrema, the data are called *the first level extrema* in the sets LMA_1 and LMI_1. Feldman [29] has addressed multi-level extrema. However, it has not given the connection with the theoretical claims.

Fig. 3(c) and (d) is another example of the multi-level extrema. Different from Fig. 3(a) and (b), this is one case that the two mono-components are treated as one IMF by the EMD. One clear difference of Fig. 3(c), (d) and Fig. 3(a), (b) is that the distributing of their extrema between the first level and the second level. For example, the data of $LMA_{1,max}$ are adjacent to the data of $LMI_{1,max}$ in Fig. 3(a) and (b). However, the data of $LMA_{1,max}$ are adjacent to the data of $LMI_{1,min}$ in Fig. 3(c) and (d). More details will be addressed about this question in Section 4.

Iterating the extraction of the extrema from the first level extrema, we can get one binary tree structure of these sets for these extrema as shown in Fig. 4.

4. Propositions

In this section some propositions are presented to show the relations between two-level extrema and the performance of EMD. These conclusions not only can help us determine what case it is, but also can help us find solutions to different cases.

Proposition 2. *In the two-level extrema of the multi-component* $x(t)(x_1(t)+x_2(t))$*, any one value in* $LMA_{1,max}$ *is always closely adjacent to one value of* $LMI_{1,max}$ *and there are no first level extrema in the interval of them, and any one value in* $LMA_{1,min}$ *is closely always adjacent to one value of* $LMI_{1,min}$ *and there are no first level extrema in the interval of them, then the two mono-components* $x_1(t)$, $x_2(t)$ *in the multi-component* $x(t)$ *can be separated well by EMD.*

For example in Fig. 3(a) and (b), every value (belonging to $LMA_{1,max}$) labeled by blank circle is always adjacent to one value (belonging to $LMA_{1,min}$) labeled by dotted and gray circle. In the interval of them there are no first level extrema. Similarly, every value (belonging to $LMI_{1,min}$) labeled by dark circle is always adjacent to one value (belonging to $LMA_{1,min}$) labeled by dotted circle. In the interval of them there are also no first level extrema. For the Proposition 2, the Proposition 1 (B) is the very case.

Proposition 3. *In the two-level extrema of the multi-component* $x(t)(x_1(t)+x_2(t))$*, any one value in* $LMA_{1,max}$ *is always closely adjacent to one value of* $LMI_{1,min}$ *and there are no first level extrema in the interval of them, and any one value in* $LMA_{1,min}$ *is always closely adjacent to one value of* $LMI_{1,max}$ *and there are no first level extrema in the interval of them, then the two mono-components in the multi-component can be treated as one IMF by EMD.*

For the Proposition 3, the corresponding theoretical condition is the Proposition 1 (C).

Definition 2. In the two-level extrema of the multi-component $x(t)(x_1(t)+x_2(t))$, if one value in $LMA_{1,max}$ is closely adjacent to one value of $LMI_{1,max}$ and there are no first level extrema in the interval of them (or one value in $LMA_{1,min}$ is always adjacent to one value of $LMI_{1,min}$ and there are no first level extrema in the interval of them), the two values of this case are called one *desired extrema couple* (*DEC*). Instead, if one value in $LMA_{1,\max}$ is closely adjacent to one value of $LMI_{1,min}$ and there are no first level extrema in the interval of them (or one value in $LMA_{1,min}$ is always adjacent to one value of $LMI_{1,max}$ and there are no first level extrema in the interval of them), the two values of this case are called one *non-desired extrema couple* (*NDEC*).

Therefore, the Propositions 2 and 3 are also expressed in the following manners (shown as the Proposition 2′ and the Proposition 3′).

Proposition 2′. *In the two-level extrema of the multi-component* $x(t)(x_1(t)+x_2(t))$*, the number of the* DEC *is non-zero and the global number of the* NDEC *is zero, then the two mono-components* $x_1(t)$, $x_2(t)$ *in the multi-component* $x(t)$ *can be separated well by EMD.*

Proposition 3′. *In the two-level extrema of the multi-component* $x(t)(x_1(t)+x_2(t))$*, the number of the* DEC *is zero and the global number of the* NDEC *is non-zero, then the two mono-components in the multi-component can be treated as one IMF by EMD.*

Therefore, in practice the Propositions 2′ and 3′ are often used instead of the Propositions 2 and 3.

Proposition 4-1. *In the two-level extrema of the multi-component* $x(t)(x_1(t)+x_2(t))$*, in any local time interval* $[T_{l_1},T_{l_2}]\subseteq[0,T]$ *the number of the* DEC *is larger than the local number of the* NDEC*, then the two mono-components* $x_1(t)$*,* $x_2(t)$ *in the multi-component* $x(t)$ *can be separated well by EMD.*

Proposition 4-2. *In the two-level extrema of the multi-component* $x(t)(x_1(t)+x_2(t))$*, in any time interval* $[T_{l_1},T_{l_2}]\subseteq[0,T]$ *the local number of the* DEC *is smaller than the local number of the* NDEC*, then the two mono-components* $x_1(t)$*,* $x_2(t)$ *in the multi-component* $x(t)$ *cannot be separated well by EMD.*

One simple method is to divide the surpport $[0,T]$ into small intervals, and in every interval we account the numbers of the *DEC* and *NDEC* respectively. Generally, every interval at least includes one *DEC* and one *NDEC*. We find that the optimal total number of the *DEC* and the *NDEC* in every interval is 5. For example, if there are 3 (or more than 3) *DEC*s and 2 (or less than 2) *NDEC*s, then the signal in this interval can be separated well by EMD. Instead, if there are 3 (or more than 3) *NDEC*s and 2 (or less than 2) *DEC*s, then the signal in this interval cannot be separated well by EMD.

These claims have been supported by the numerical experiments. Appendix A gives three tables showing these relations. The first table (Table A1) is the result of two tones whose frequencies are constant. In the second table (Table A2) it is the result of two chirps. Table A3 give the result of two signals whose frequencies are quadratic polynomials. Without loss of generalization, all the amplitudes of the six signals are equal to 1. The first observation is that when the frequency ratio $f_1(t)/f_2(t)(f_1(t)>f_2(t))$ increases, the *DEC* increase and the *NDEC* decrease simultaneously relatively. The measurement quantity $c(t)$ decreases from 1 to 0 gradually. This means that the ratio $(a_1(t)f_1(t))/(a_2(t)f_2(t))$ (because $a_1(t)=a_2(t)=1$ here) is more larger, the better the multi-component will be decomposed by EMD. The second observation is that when the ratio $f_1/f_2\approx 1.5$, the *DEC*s are not zeroes any longer. It will become one non-zero number. The ratio 1.5 turn out to be one threshold. The third observation is that when the ratio $f_1/f_2=2$, the *DEC*s are equal to the *NDEC*s (or at most different by one). This means that the ratio 2 is one threshold. The fourth observation is that when the ratio $f_1/f_2\approx 3$, the *NDEC*s become zeroes, when there are only *DEC*s left. This means that the ratio 3 is also one threshold. These tables turn out to be in good agreement with intuition and physical interpretation shown in the Propositions 1 and 2–4. These tables have supported our propositions.

The above Propositions 2–4 can help us to decide whether the multi-component can be separated well or not by EMD and then tell us what the EMD will do in practice.

5. Improved EMD

5.1. Cases I, II and III

Using the Propositions 2–4, we know when the Multi-component signal cannot be separated by EMD in practice. After knowing the cases, the next step is to find new way to separate the Multi-component signal into the FM mono-components. Now our improved EMD are as follows.

(S1) Extract the first level extrema, including the local maxima and minima, and the second level extrema of the Multi-component signal $x(t)$.
(S2) Using Propositions 2–4 to decide which case it is.
(S3) If it is *Case* I, then use EMD to obtain $imf_1(t)$. Turn to S6.
(S4) If it is *Case* II, then
1. Use EMD to obtain $imf_{1,0}(t)$;
2. Find the extrema's locations t_{ex} of $imf_{1,0}(t)$ to construct the set $L_{ex}=\{t_{ex}\}$;
3. Use the least-squares method to estimate the phase polynomial $\varphi(t)$. Where $\varphi(t)$is the phase of $y(t)=\cos\varphi(t)$,$y'(t_{ex})=-\varphi'(t_{ex})\sin\varphi(t_{ex})=0$ (or $y(t_{ex})=\pm 1$);
4. Use formulations (7) and (8) to estimate the amplitude, $a_{1,0}$, of the FM component $tx_1(t)$ to get $a_{1,0}\cos\varphi(t)$;
5. Use the formulation (9) to obtain the final amplitude estimation $a_{1,opt}$ based on $a_{1,0}\cos\varphi(t)$;
6. $imf_1(t)=a_{1,opt}\cos\varphi(t)$;
7. Turn to S6.

(S5) If it is *Case* III, then
1. Use EMD to obtain $imf_{1,0}(t)$;
2. Interpolate the maxima and minima of $imf_{1,0}(t)$ to get the up and down envelopes $EV_{up}(t)$ and $EV_{down}(t)$ to get the initial amplitude $a_{1,0}=(1/T)\sum_t\left[\left(|EV_{up}(t)|+|EV_{down}(t)|\right)/2\right]$,$(t\in[0,T])$;
3. Find the extrema's locations t_{ex} of $imf_{1,0}(t)$ to construct the set $L_{ex}=\{t_{ex}\}$;
4. Use the least-squares method to estimate the phase polynomial $\varphi(t)$. Where $\varphi(t)$ is the phase of $y(t)=\cos\varphi(t)$ and$y'(t_{ex})=-\varphi'(t_{ex})\sin\varphi(t_{ex})=0$ (or $y(t_{ex})=\pm 1$);

5. Use the formulation (9) to obtain the final amplitude estimation $a_{1,opt}$ based on $a_{1,0}\cos\varphi(t)$;
6. $imf_1(t)=a_{1,opt}\cos\varphi(t)$;
7. Turn to S6.

(S6) $res(t)=x(t)-imf_1(t)$. Use $res(t)$ instead of $x(t)$ to repeat the steps S1–S6 until the residue $res(t)$ is lower than a threshold value, thd_2, of error tolerance.

The improved EMD is based on EMD. For the *Case* II and *Case* III, one IMF should be obtained using EMD first. For *Case* II, the IMF is one AM–FM signal approximately. For *Case* III, the IMF is one mixture of one AM–FM signal and one FM signal, i.e., the IMF contains the whole $x_1(t)$ and one part of $x_2(t)$. If it is *Case* I, only the EMD is sufficient. Note that the difference of the *Case* II and *Case* III is the calculation of the initial amplitudes. Only for the AM–FM signal, the initial amplitude can be estimated using formulations (7) and (8). Instead, for the non-AM–FM signal in *Case* III, the mean of the envelopes of the first IMF will work well.

Using the least-squares method to obtain the phase polynomial $\varphi(t)$ is easily realized. For the given maximal power n of the phase polynomial $\varphi(t)=\sum_{l=0}^{n}b_l t^l$, using $y'(t_{ex})=-\varphi'(t_{ex})\sin\varphi(t_{ex})=0$ (or $y(t_{ex})=\pm1$) to estimate the coefficients b_l $(l=0,\ldots,n)$ of $\varphi(t)$ is very fitting (see Appendix B). Generally we will set maximal power n larger.

5.2. The other case—Case IV

The former cases has the condition $a_1(t)f_1(t)>\approx a_2(t)f_2(t)$. In these cases, the extrema rate is exactly the same as that of the first FM component [5]. There is one case that the extrema rate is exactly the same as that of the second FM component. In this case all the Propositions 2–4 and the improved approaches addressed above will not work any longer. For example, Fig. 5 is one classical example of this case. The two FM components are included in the same one IMF.

In the following there is the resolution of this case.

C1. Use the improved EMD approach defined in steps S1–S6 to obtain all the IMFs: $imf_l(t)(l=1,\ldots,N)$.
C2. Find the extrema's locations t_{ex} of $imf_l(t)$ to construct the set $L_{ex}=\{t_{ex}\}$.
C3. Interpolate the maxima and minima of $imf_l(t)$ to get the up and down envelopes $EV_{up}(t)$ and $EV_{down}(t)$ to get the initial amplitude $a_{l,0}=(1/T)\sum_t\left[\left(|EV_{up}(t)|+|EV_{down}(t)|\right)/2\right](t\in[0,T])$.
C4. Use the least-squares method to estimate the phase polynomial $\varphi(t)$. Where $\varphi(t)$is the phase of $y(t)=\cos\varphi(t)$ and $y'(t_{ex})=-\varphi'(t_{ex})\sin\varphi(t_{ex})=0$ (or $y(t_{ex})=\pm1$).
C5. Use the formulation (9) to obtain the final amplitude estimation $a_{l,opt}$ based on $a_{l,0}\cos\varphi(t)$.
C6. One new IMF is obtained: $imf_{l,new}(t)=imf_l(t)-a_{l,opt}\cos\varphi(t)$.
C7. If $\|imf_{l,new}(t)\|_{L^2(R)}/\|imf_l(t)\|_{L^2(R)}<threshold$, there is no hidden component in the IMF. Otherwise, repeat steps C1–C6 on $imf_{l,new}(t)$ instead of $imf_l(t)$ until $\|imf_{l,new}(t)\|_{L^2(R)}\|imf_l(t)\|_{L^2(R)}<threshold$ holds. Here we let $threshold=0.01$.
C8. Reorder all the IMFs including the old and new ones according to their frequencies.

Different with the improved approaches of *Case* II and *Case* III, here the estimated component $a_{l,opt}\cos\varphi(t)$ is the low-frequency FM component in the IMF $imf_l(t)$. The *threshold* is given in advance and empirical. This means if the energy of the $imf_{l,new}(t)$ is less than 1% of that of $imf_l(t)$, the program of searching the high-frequency low-energy component will end.

Therefore, our full improved EMD includes the steps S1—S8 and steps C1–C8. The steps C1–C8 should be performed after the steps S1–S8. Sometimes, if we have *a priori* that there is no *Case* IV existing in the Multi-component signal, only the steps C1–C8 are needed.

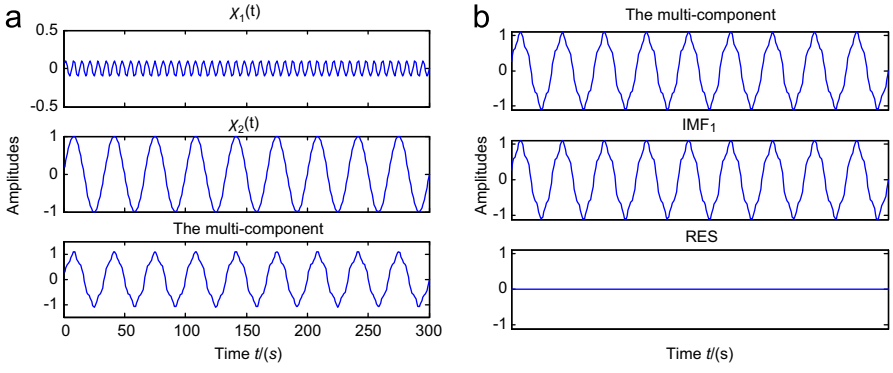

Fig. 5. Decomposition of one FM multi-component using EMD. (a) From top to bottom: $x_1(t)$, $x_2(t)$ and the comprised component $x(t)$ (b) From top to bottom: $x(t)$, $imf_1(t)$ and $res(t)$ using EMD.

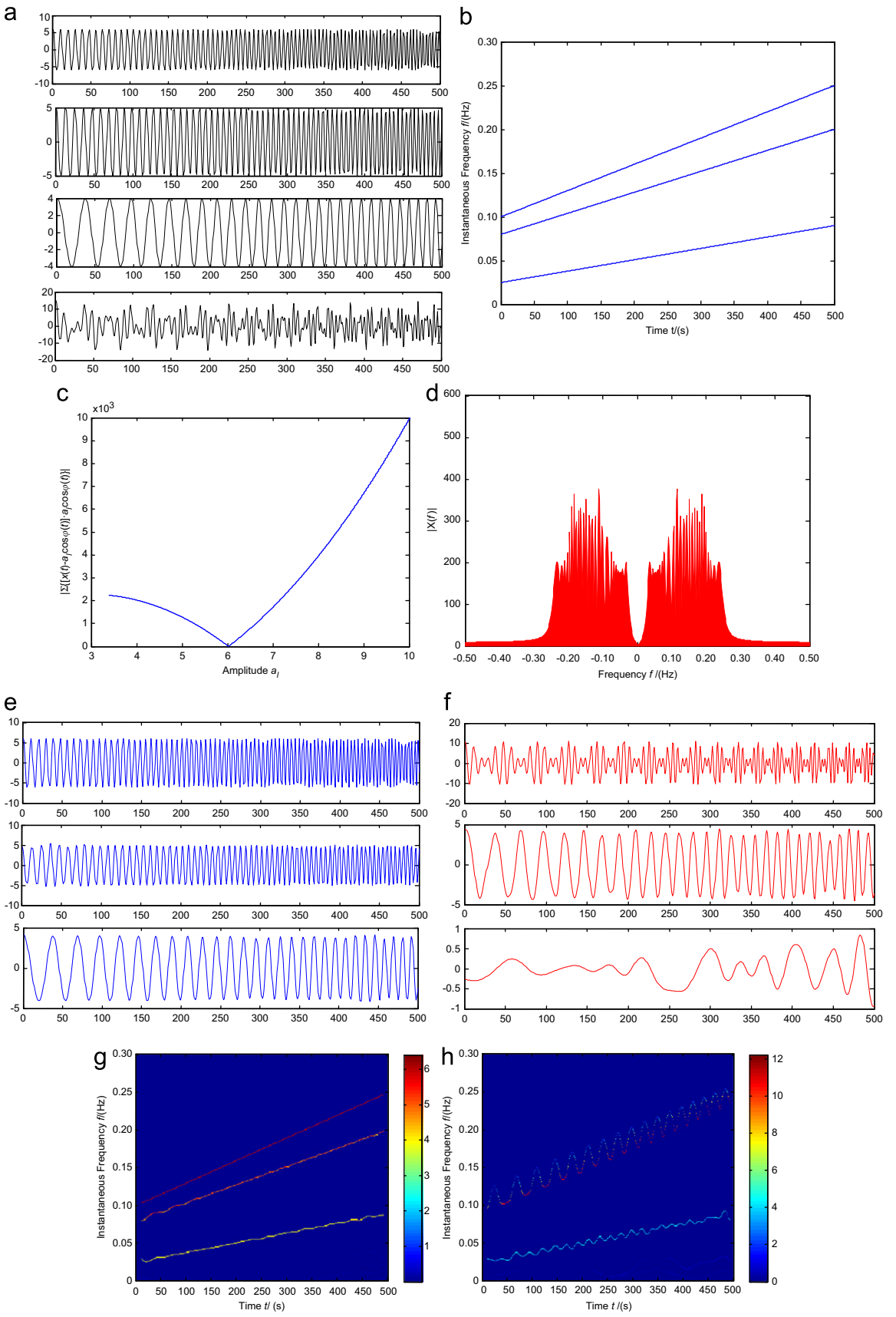

Fig. 6. The analysis of three chirps using our method and EMD. (a) From top to bottom: x1(t), x2(t), x3(t) and the comprised component x(t). (b) Real t-f distribution of x(t). (c) Optimal estimation of amplitude (d) FFT of x(t) (e) From top to bottom: imf1(t), imf2(t), imf3(t) using our method. (f) From top to bottom: imf1(t), imf2(t), imf3(t) using EMD. (g) t-f distribution of our method. (h) t-f distribution of EMD.

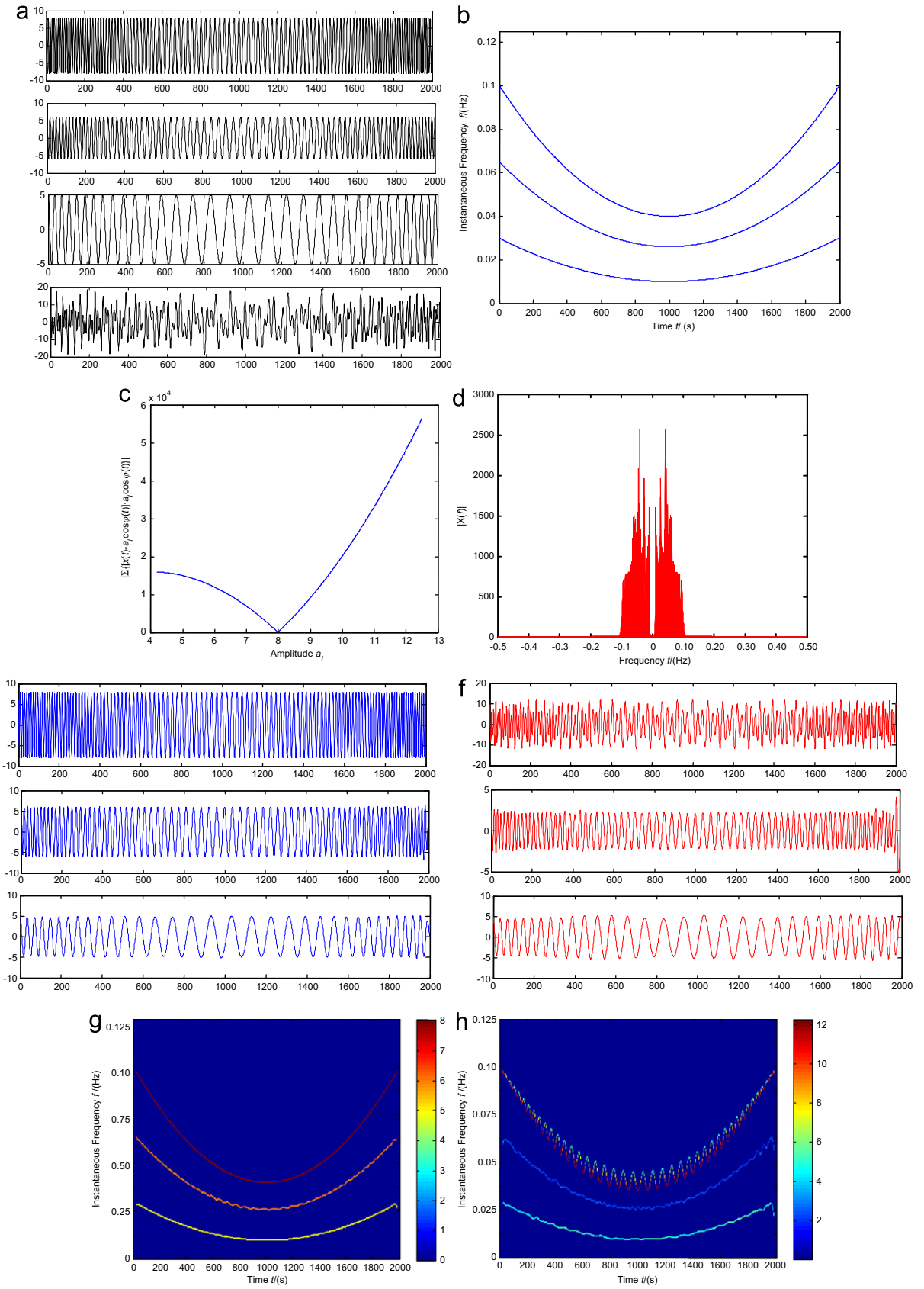

Fig. 7. The analysis of three quadratic-FM components using our method and EMD. (a) From top to bottom: x1(t), x2(t), x3(t) and the comprised component x(t). (b) Real t-f distribution of x(t). (c) Optimal estimation of amplitude (d) FFT of x(t) (e) From top to bottom: imf1(t), imf2(t), imf3(t) using our method. (f) From top to bottom: imf1(t), imf2(t), imf3(t) using EMD. (g) t-f distribution of our method. (h) t-f distribution of EMD.

6. Demonstration

The ability of our improved EMD to separate the FM components from the multi-component is demonstrated in this section. Three tests are presented: the first test involves three chirps and the second test involves three quadratic-FM components, and the last test also involves three chirps. The sampling frequency involved in the three tests is 1 Hz. The maximal power n of phase polynomial $\varphi(t)$ involved in the three tests is 4. $threshold=0.01$, $thd_1=2000$, $thd_2=0.01$.

6.1. Test one

In this section, the test is used to validate the improved method defined in steps S1–S4 and S6. The three chirps are defined as $x_l(t)=a_l\cos\varphi_l(t)$, $\varphi_l'(t)/2\pi=f_l(t)$ $(l=1,2,3)$. The three chirps and their multi-component $x(t)=a\cos\varphi(t)=\sum_{l=1}^{3}a_l\cos\varphi_l(t)$ are shown as Fig. 6(a). Their frequencies and amplitudes have the following relations: $a_1f_1(t)>a_2f_2(t)$, $2f_2(t)>f_1(t)>1.5f_2(t)$, $a_2f_2(t)>a_3f_3(t)$, $f_2(t)>2f_3(t)$. Note that the relations will exclude the using of the step S5. The three amplitudes are 6, 5 and 4, respectively. In this test the time support is 500 s. As shown in Figs. 6(b), $f_1(t)\in[0.1,0.25]$, $f_2(t)\in[0.08,0.20]$ and $f_3(t)\in[0.025,0.09]$. The FFT$X(f)$, of the comprised multi-component, $x(t)$, is shown in Fig. 6(d), which shows that the three chirps' spectrums cannot be separated using their Fourier transform. In addition, there are no distinctive frequency peaks. For this case, the masking signal based EMD [7,8] will not work because there are no fitting frequency components found from their FFT for masking signals.

Instead, our improved method can separate the three chirps effectively, as shown in Fig. 6(e). For the first component, the optimal amplitude estimation $a_{1,opt}$ is 6.0450, as shown in Fig. 6(c). The decomposed results of EMD are shown in Fig. 6(f)–(h) are the t–f distributions of the decomposed results using our method and EMD, respectively. Compared with the real t–f distribution, one main component has been missed by EMD. Alternately, the two FM components have been taken as one IMF using EMD.

6.2. Test two

In this section, the test is used to validate the improved method defined in steps S1, S2, S3, S5 and S6. Different with the first test, there are three quadratic-FM components. The three components shown in Fig. 7(a) have the following relations: $a_1f_1(t)>a_2f_2(t)$, $1.5f_2(t)>f_1(t)>f_2(t)$, $a_2f_2(t)>a_3f_3(t)$, $f_2(t)>2f_3(t)$, which will exclude the using of the step S4. Their amplitudes are 8, 6 and 5, respectively. In this test the time support is 2000 s. As shown in Fig. 7(b), $f_1(t)\in[0.04,0.10]$, $f_2(t)\in[0.026,0.065]$ and $f_3(t)\in[0.01,0.03]$. The FFT, $X(f)$, of the comprised multi-component, $x(t)$, is shown in Fig. 7(d), which shows that the three quadratic-FM components' spectrums cannot be separated using their Fourier transform. In addition, there are no distinctive frequency peaks. The masking signal based EMD [7,8] will not work under this case. Fig. 7(e) is the decomposed result using our improved method. For the first component, the optimal amplitude estimation $a_{1,opt}$ is 7.9940, as shown in Fig. 7(c). The decomposed results of EMD are shown in Fig. 7(f). Fig. 7(g) and (h) are the t–f distributions of the decomposed results using our method and EMD, respectively. Clearly, the first IMF of EMD not only contains the first FM component $x_1(t)$, but also contains one part of the second FM component $x_2(t)$, i.e., $0<b(t)<1$ (where $imf_1(t)=x_1(t)+b(t)x_2(t)$). This result can be also found from the two t–f distributions, as shown in Fig. 7(g) and (h), compared with the real t–f distribution shown in Fig. 7(b).

6.3. Test three

In this section, the test is used to validate the improved method defined in steps S1, S2, S3, S6 and C1–C8. The three chirps and their multi-component are shown as Fig. 8(a). Their frequencies and amplitudes have the following relations: $a_1f_1(t)<a_2f_2(t)$, $f_1(t)>2f_2(t)$, $a_2f_2(t)>a_3f_3(t)$, $f_2(t)>2f_3(t)$. Note that the relations will exclude the using of the steps S4 and S5. The three amplitudes are 2, 6 and 5, respectively. In this test the time support is 300 s. As shown in Fig. 7(b), $f_1(t)\in[0.15,0.40]$, $f_2(t)\in[0.12,0.32]$ and $f_3(t)\in[0.04,0.12]$. The FFT of the comprised multi-component is shown in Fig. 7(c), which shows that the three chirps' spectrums cannot be separated using their Fourier transform. Similar with the former two tests, the masking signal based EMD [7,8] will not work here. Compared with the real t–f distribution (Fig. 8(b)) and our result (Fig. 8(d)), the t–f distribution of EMD in Fig. 8(e) has missed one component, and the two FM components have been taken as one IMF using EMD.

6.4. Relation between phase polynomial and amplitude estimation

In the steps S4 and S5 of our improved EMD, there is an important potential relation between the phase polynomial and the amplitude estimation. If the estimated phase polynomial using the least-squares method is very different from the actual phase polynomial, then there maybe be no optimal amplitude. Therefore, the maximal power n of the phase polynomial $\varphi(t)$ should be increased if there is no optimal amplitude found using the initial given power n through the formulation (9). If there is no any prior knowledge about the maximal power n of the phase polynomial $\varphi(t)$, the initial given power n should be initialized using one bigger number.

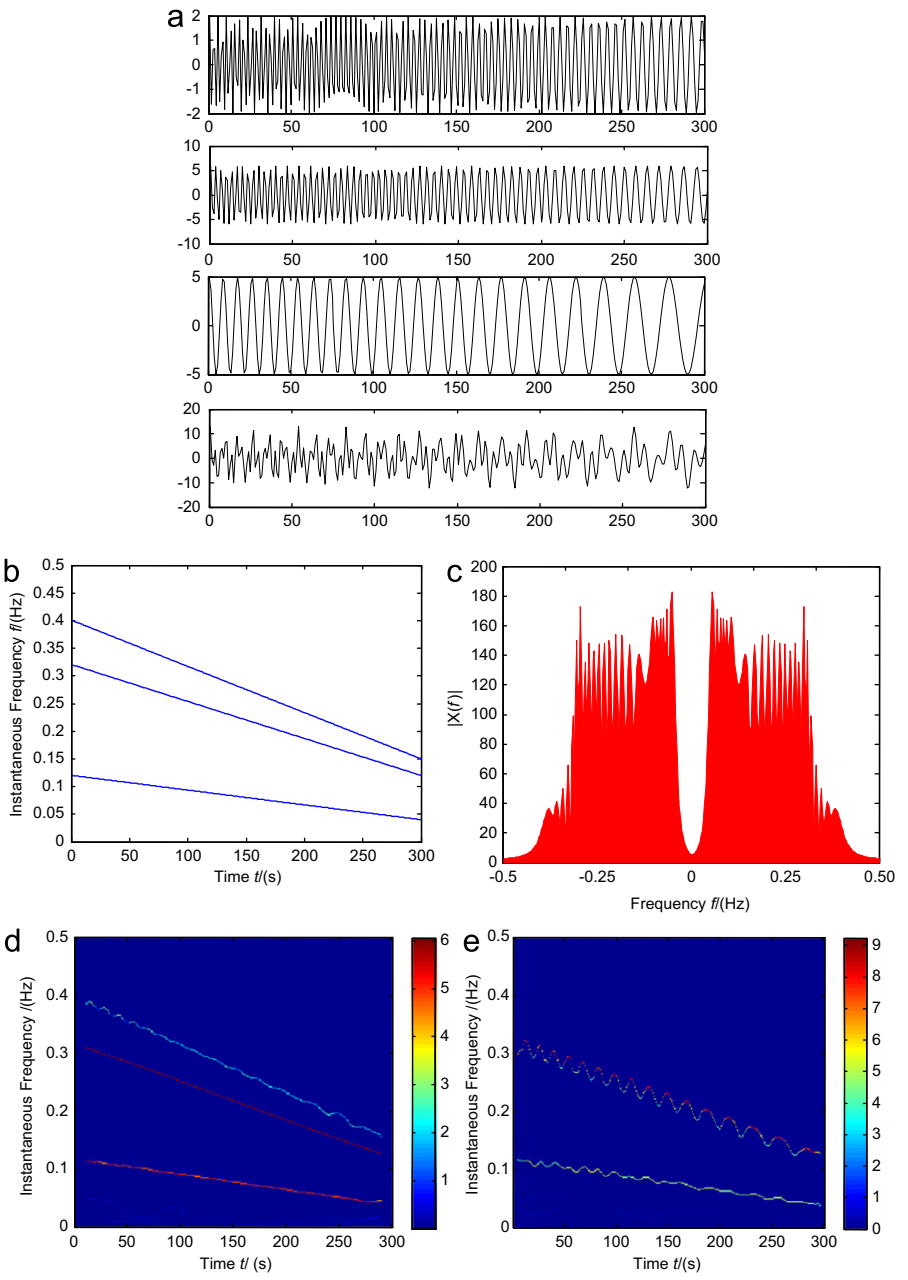

Fig. 8. The analysis of three chirps using our method and EMD. One component's extrema are invisible in the multi-component. (a) From the top to bottom: x1(t), x2(t), x3(t) and their comprised component. (b) Real t-f distribution of x(t) (c) FFT of x(t) (d) t-f distribution of our method (e) t-f distribution of EMD.

Table 1 gives the relation between the initial given power n and the optimal amplitude estimation for the first component in Figs. 6 and 7. " $\times$ " denotes that there is no optimal estimated amplitude found using the formulation (9). This means that the initial given power must be bigger than the actual power by one at least. It is also shown that different power has no distinctive different effect on the estimated amplitude from Table 1. Table 2 gives the optimal amplitude estimation with different Gaussian noises (the power n is 4 in this experiment), as shown by the performance of anti-noise via optimization.

7. Conclusion

In this paper, a novel algorithm of improved EMD has been presented for the analysis of FM signals. First, extract the first level extrema and the second level extrema to construct one two-level extrema structure. Using the locations'

Table 1
The relation between the initial given power n and the optimal amplitude estimation.

Estimated amplitude	The given maximal power n									
	1	2	3	4	5	6	7	8	9	10
Fig. 6	×	6.0310	6.0300	6.0450	6.0420	6.0500	6.0350	6.0320	5.9930	5.9090
Fig.7	×	×	7.9980	7.9940	7.9940	7.9880	7.9890	7.9870	7.9910	7.9800

Table 2
The optimal amplitude estimation with different Gaussian noises (the power n is 4 in this experiment).

Estimated amplitude	The given Gaussian variance									
	0.1	0.2	0.3	0.4	0.5	0.6	0.7	0.8	0.9	1
Fig. 6	6.0550	6.1310	5.8300	6.2087	6.3213	6.3500	5.6350	6.5320	6.5912	5.5090
Fig.7	7.9910	7.9340	8.1980	7.8943	7.7934	7.6870	7.6121	7.5073	8.4910	7.4302

Table A1

f_1/f_2	*DEC*	*NDEC*	$c(t)$
1.0256	0	9	0.9999
1.0526	0	20	0.9995
1.0811	0	30	0.9987
1.1111	0	39	0.9968
1.1429	0	50	0.9939
1.1765	0	60	0.9855
1.2121	0	69	0.9794
1.2500	0	78	0.9566
1.2903	0	89	0.9377
1.3333	0	99	0.9081
1.3793	0	109	0.8763
1.4286	0	118	0.7083
1.4815	***0***	***129***	***0.4353***
1.5385	***18***	***138***	***0.2338***
1.6000	48	147	0.1078
1.6667	79	159	0.0696
1.7391	108	167	0.0374
1.8182	137	178	0.0206
1.9048	169	189	0.0217
2.0000	***197***	***198***	***0.0034***
2.1053	188	167	0.0024
2.2222	179	139	0.0007
2.3529	168	108	0.0011
2.5000	157	78	0.0005
2.6667	149	49	0.0007
2.8571	***137***	***18***	***0.0002***
3.0769	***128***	***0***	***0.0003***
3.3333	119	0	0.0000
3.6364	108	0	0.0003
4.0000	99	0	0.0002
4.4444	89	0	0.0002
5.0000	79	0	0.0001
5.7143	68	0	0.0001
6.6667	59	0	0.0000
8.0000	50	0	0.0000
10.0000	40	0	0.0000

Note: The bold forms denote the thresholds.

relations between the first level extrema and the second level extrema, we know what EMD does for the FM signals in practice. There are four cases involved for the analysis of FM signals. For the first case, EMD is sufficient. For the other three cases, different improved methods are presented to separate the components that EMD cannot separate. The least-squares method is used to estimate the phase polynomial. The orthogonal relations between different components are used to estimate the optimal amplitudes of FM components. Finally, three different experiments are given to show our new

improved EMD. Note that our method still holds for signals whose frequencies are stationary equivalents, because these signals are special FM components.

Our future work will include how these methods can be generalized into more general and more complex cases.

Acknowledgment

This work was supported by the NSFCs (nos. 60975016 and 61002052).

Appendix A

Three tables showing the relations between frequency ration, *DEC*/*NDEC* and measurement $c(t)$. (Tables A1–A3).

Appendix B

Let $y(t)=\cos\varphi(t)+g(t)$ (where $g(t)$ is the zero-mean Gaussian noise),$\varphi(t)=\sum_{l=0}^{n} b_l t^l+\varphi_g(t)$ ($\varphi_g(t)$) is the phase noise by $g(t)$). For $t_{ex}=\{t_{ex,1},t_{ex,2},\ldots,t_{ex,m}\}$, $y(t_{ex,n})=1$ and $y(t_{ex,n+1})=-1$ (FM component has the constant amplitude), where n is odd and n, $n+1\le m$.

Then we have

$$\varphi(t_{ex,n})=(n+1)\pi \tag{11}$$

Therefore through minimizing $\|Ab-\Phi\|_2^2$ to get the optimal coefficients

$$b=(A^TA)^{-1}A^T\Phi \tag{12}$$

Table A2

f_1/f_2	*DEC*	*NDEC*	$c(t)$
1.0256	0	7	1.0000
1.0526	0	15	1.0000
1.0811	0	22	0.9995
1.1111	0	30	0.9968
1.1429	0	37	0.9925
1.1765	0	45	0.9872
1.2121	0	51	0.9802
1.2500	0	59	0.9574
1.2903	0	67	0.9370
1.3333	0	74	0.9249
1.3793	0	82	0.8761
1.4286	1	89	0.6926
1.4815	***1***	***95***	***0.4546***
1.5385	***15***	***101***	***0.2610***
1.6000	36	110	0.1409
1.6667	58	118	0.0778
1.7391	79	126	0.0377
1.8182	102	132	0.0182
1.9048	124	141	0.0188
2.0000	***148***	***148***	***0.0108***
2.1053	141	125	0.0087
2.2222	133	103	0.0026
2.3529	126	79	0.0008
2.5000	117	60	0.0011
2.6667	111	37	0.0010
2.8571	***103***	***13***	***0.0003***
3.0769	***97***	***0***	***0.0001***
3.3333	89	0	0.0001
3.6364	82	0	0.0002
4.0000	74	0	0.0002
4.4444	66	0	0.0001
5.0000	58	0	0.0001
5.7143	50	0	0.0001
6.6667	45	0	0.0062
8.0000	37	0	0.0003
10.0000	30	0	0.0000

Note: The bold forms denote the thresholds.

Table A3

f_1/f_2	*DEC*	*NDEC*	$c(t)$
1.0256	0	6	1.0000
1.0526	0	13	0.9999
1.0811	0	19	0.9987
1.1111	0	26	0.9971
1.1429	0	33	0.9931
1.1765	0	39	0.9862
1.2121	0	46	0.9801
1.2500	0	53	0.9553
1.2903	0	59	0.9384
1.3333	0	66	0.9269
1.3793	0	72	0.8761
1.4286	0	79	0.7441
1.4815	***0***	***86***	***0.4676***
1.5385	***13***	***92***	***0.2219***
1.6000	32	99	0.1306
1.6667	52	105	0.0775
1.7391	73	112	0.0354
1.8182	92	119	0.0181
1.9048	112	125	0.0074
2.0000	***87***	***88***	***0.0019***
2.1053	125	112	0.0018
2.2222	119	92	0.0010
2.3529	112	73	0.0008
2.5000	105	52	0.0006
2.6667	99	32	0.0011
2.8571	***92***	***13***	***0.0003***
3.0769	***86***	***0***	***0.0003***
3.3333	79	0	0.0008
3.6364	72	0	0.0003
4.0000	66	0	0.0002
4.4444	59	0	0.0003
5.0000	53	0	0.0003
5.7143	46	0	0.0002
6.6667	39	0	0.0001
8.0000	33	0	0.0000
10.0000	26	0	0.0060

Note: The bold forms denote the thresholds.

$$\text{where } b=\begin{bmatrix} b_l \\ b_{l-1} \\ \vdots \\ b_1 \\ b_0 \end{bmatrix}, \quad A=\begin{bmatrix} t_{ex,1}^{l} & t_{ex,1}^{l-1} & \cdots & t_{ex,1} & 1 \\ t_{ex,2}^{l} & t_{ex,2}^{l-1} & \cdots & t_{ex,2} & 1 \\ \cdots & \cdots & \cdots & \cdots & \cdots \\ t_{ex,m}^{l} & t_{ex,m}^{l-1} & \cdots & t_{ex,m} & 1 \end{bmatrix}, \text{ and } \Phi=\begin{bmatrix} 2\pi \\ 3\pi \\ \vdots \\ m\pi \\ (m+1)\pi \end{bmatrix}.$$

References

[1] N.E. Huang, S. Zheng, R.L. Steven, et al., The empirical mode decomposition and the Hilbert spectrum for nonlinear non-stationary time series analysis, Proc. R. Soc. London Ser. A 454 (1998) 903–995.
[2] A.O. Boudraa, J.C. Cexus, EMD-based signal filtering, IEEE Trans. Instrum. Meas. 56 (6) (2007) 2196–2202.
[3] H.L. Liang, Q.H. Lin, J.D.Z. Chen, Application of the empirical mode decomposition to the analysis of esophageal manometric data in gastroesophageal reflux disease, IEEE Trans. Biomed. Eng. 52 (10) (2005) 1692–1701.
[4] H. Liang, Z. Lin, R.W. McCallum, Artifact reduction in electrogastrogram based on empirical mode decomposition method, Med. Biol. Eng. Comput. 38 (2000) 35–41.
[5] C. Han, G.H. Wang, C.D. Fan, A novel method to reduce speckle in SAR images, Int. J. Remote Sensing 23 (23) (2002) 5095–5101.
[6] G.L. Xu, X.T. Wang, X.G. Xu, Neighborhood limited empirical mode decomposition and application in image processing, in: ICIG, 2007, Chengdu of China, pp. 149–154.
[7] J.C. Nunes, Y. Bouaoune, E. Delechelle, et al., Texture analysis based on the bidimensional empirical mode decomposition with gray-level co-occurrence models, IEEE Mach. Vision Appl. 2 (2003) 633–635.
[8] A.R. Messina, V. Vittal, Extraction of dynamic patterns from wide-area measurements using empirical orthogonal functions, IEEE Trans. Power Syst. 22 (2) (2007) 1843–1850.
[9] N. Bi, Q.Y. Sun, D. Huang, Z.H. Yang, J. Huang, Robust image watermarking based on multiband wavelets and empirical mode decomposition, IEEE Trans. Image Process. 16 (8) (2007) 1956–1966.
[10] Y.F. Zhang, Y.L. Gao, L. Wang, J.H. Chen, X.L. Shi, The removal of wall components in Doppler ultrasound signals by using the empirical mode decomposition algorithm, IEEE Trans. Biomed. Eng. 54 (9) (2007) 1631–1642.
[11] Tao Qian, Mono-components for decomposition of signals, Math. Methods Appl. Sci. 29 (2006) 1187–1198.
[12] Wang Xu Guanlei, Xu Xiaogang. Xiaotong, Time-varying frequency-shifting signal assisted empirical mode decomposition method for AM–FM signals, Mech. Syst. Signal Process. 23 (8) (2009) 2458–2469.

[13] G. Rilling, P. Flandrin, On the influence of sampling on the empirical mode decomposition, in: Proceedings of the IEEE International Conference on Acoustics, Speech and Signal Processing (ICASSP), 2006, pp. 444–447.
[14] R.C. Sharpley, V. Vatchev, Analysis of the intrinsic mode functions, Construct. Approx. 24 (2006) 17–47.
[15] P. Flandrin, G. Rilling, P. Gonçalvés, Empirical mode decomposition as a filter bank, IEEE Signal Process. Lett. 11 (2) (2004) 112–114.
[16] P. Flandrin, P. Gonçalvés, Empirical mode decompositions as data-driven wavelet-like expansions for stochastic processes, Int. J. Wavelets Multires. Inf. Process. 2 (4) (2004) 477–496.
[17] G. Rilling, P. Flandrin, One or two frequencies? The empirical mode decomposition answers, IEEE Trans. Signal Process. 56 (1) (2008) 85–95.
[18] Z. Wu, N.E. Huang, A study of the characteristics of white noise using the empirical mode decomposition method, Proc. R. Soc. London A 460 (2004) 1597–1611.
[19] R. Deering, J.F. Kaiser, The use of a masking signal to improve empirical mode decomposition, in: IEEE, ICASSP 2005, IV, pp. 485–488.
[20] N. Senroy, S. Suryanarayanan, Paulo F. Ribeiro, An improved Hilbert–Huang method for analysis of time-varying waveforms in power quality, IEEE Trans. Power Syst. 22 (4) (2007) 1843–1850.
[21] W.P. Torres, A.V. Oppenheim, R.R. Rosales, Generalized frequency modulation, IEEE Trans. Circuits Syst. I: Fundam. Theory Appl. 48 (12) (2001) 1405–1412.
[22] G. Feruz, C.L. Evans, B.G. Saar, et al., High-sensitivity vibrational imaging with frequency modulation coherent anti-Stokes Raman scattering (FM CARS) microscopy, Opt. Lett. 31 (12) (2006) 1872–1874.
[23] M.R. Pufall, W.H. Rippard, S. Kaka, T.J. Silva, et al., Frequency modulation of spin-transfer oscillators, Appl. Phys. Lett. 86 (8) (2005) 506–508.
[24] E.A. Whittaker, J.F. Kelly, S.W. Sharpe, et al., Wideband frequency modulation spectroscopy using the quantum cascade laser, in: Internal Conference on Lasers and Electro-Optics, 1999, pp.194–195.
[25] I. Vincent, F. Auger, C. Doncarli, A comparative study between two instantaneous frequency estimators, in: Proceedings of the Eusipco-94, vol. 3, 1994, pp. 1429–1432.
[26] P. Djuric, S. Kay, Parameter estimation of chirp signals, IEEE Trans. Acoust. Speech Signal Process. 38 (12) (1990).
[27] S.M. Tretter, A fast and accurate frequency estimator, IEEE Trans. ASSP 37 (12) (1989) 1987–1990.
[28] Time–frequency toolbox for use with matlab, available at: 〈http://tftb.nongnu.org/tutorial.pdf〉.
[29] M. Feldman, Non-linear free vibration identification via the Hilbert transform, J. Sound Vib. 208 (3) (1997) 475–489.